Chapter 8

Modeling of Coupled Memristive-Based Architectures Applicable to Neural Network Models

Jason Kamran Jr Eshraghian, Herbert H.C. Iu and Kamran Eshraghian

Additional information is available at the end of the chapter

http://dx.doi.org/10.5772/intechopen.69327

Abstract

This chapter explores the dynamic behavior of dual flux coupled memristor circuits in order to explore the uncharted territory of the fundamental theory of memristor circuits. Neuromorphic computing anticipates highly dense systems of memristive networks, and with nanoscale devices within such close proximity to one another, it is anticipated that flux and charge coupling between adjacent memristors will have a bearing upon their operation. Using the constitutive relations of memristors, various cases of flux coupling are mathematically modeled. This involves analyzing two memristors connected in composite, both serially and in parallel in various polarity configurations. The new behavior of two coupled memristors is characterized based on memristive state equations, and memductance variation represented in terms of voltage, current, charge and flux. The rigorous mathematical analysis based on the fundamental circuit equations of ideal memristors affirms the memristor closure theorem, where coupled memristor circuits behave as different types of memristors with higher complexity.

Keywords: memristor, memductance, coupling, flux, charge, series, parallel

1. Introduction

In 1969, Leon Chua became the first person to publish non-linear circuit theory against a mathematical foundation [1]. In doing so, it became apparent that there was a hole in the circuit equations at the time. Shortly after, in 1971 he postulated that symmetry implies the existence of a fourth fundamental circuit element to link the missing relationship between charge and flux —that circuit element being the memristor [2]. This research resurfaced and was popularized in 2008, when Hewlett-Packard fabricated the first functional nanoscale memristor [3]. This particular brand of memristor was based on a bi-level titanium dioxide thin film containing dopants which migrate across the width of the memristor when a current is applied to it.

Each fundamental circuit element holds a relationship between any two of either voltage, current, charge, or flux. The memristor thus becomes a fundamental circuit element as it fills the missing gap of the charge-flux relationship. It is important to note that even though q and ϕ are referred to as charge and flux, they do not have to be associated with a physical charge or real flux as is the case with classical conductors and inductors [4]. The integrating relationship between voltage and flux results in memristors being able to retain history, and exhibiting potentially different current values when the same voltage is applied to it. By definition, this enables the memristor to have different resistance values regardless of identical voltage excitation, stemming from memristance being a function of historical voltage. This gives rise to the nomenclature surrounding the memristor, a portmanteau of 'memory resistor'.

The inherent characteristics of this revolutionary device have enabled its application in a diverse field of areas, including neuromorphic circuits [5] and non-volatile memory applications [6]. These applications often see arrays of memristors behaving compositely with one another. In addition to the functionality of single discrete memristors, the behaviors of multiple memristors in structures of connectivity have also been analyzed.

Memristors are polarity dependant—while this complicates circuit analysis, it allows for many more configuration permutations than the other fundamental circuits: the resistor, capacitor and inductor. The behavior of two memristor emulators in both serial and parallel connections are experimentally evaluated in Ref. [7], however, only identical polarity directions are considered. Two charge controlled memristors are connected in series and in parallel in Ref. [8], with their responses evaluated when polarity is varied. The composite behavior is analyzed by probing the relationships between flux, charge and memristance. The results show novel *I-V* characteristics which will prove to be useful applications in neural networks and logic circuits. The magnetic coupling of memristors are also considered in terms of mutual induction and capacitive connections in Ref. [9].

Many researchers have sought to use memristors to represent the synapses between neurons in artificial networks, and more recently, a memristive crossbar array has been successfully fabricated which implements a neural network, and is successfully capable of performing limited classifications and simple pattern recognition [10]. By training such networks on sets of known example patterns and tuning the weights of the 'synaptic' connections, unknown patterns and images can be recognized. Ultimately, researchers anticipate that networks with a density of 100 billion synapses per square centimeter in each layer should soon be possible by shrinking memristors down to 30 nm across. This indicates highly dense 3D structures with a very large number of memristors within very close proximity of one another will be the norm, and coupling memristor theory is of fundamental significance to this field. The use of memristive crossbar architectures has been gaining much traction in computing large sets of data [11–14], and the theory behind memristive coupling is absolutely essential in ensuring information is not lost due to undesirable coupling, or by manufacturing more efficient modes of information storage by utilizing coupling theory.

The coupling effects of capacitors and inductors via electric and magnetic fields are well known. The mutual capacitances and inductances of circuits comprised of multiple TiO_2 memristors are dependent upon the physical features of each memristor cell [14], such as size and position.

Therefore, coupling is to be expected between adjacent memristors, and must be taken into account when analyzing highly concentrated circuits. In addition to series and parallel connections, coupling has thus been established as a third unique relation in memristive systems [15].

The behavior of coupled memristors was rigorously analyzed in a systematic manner for the first time in Ref. [16] with consideration given to all polarity combinations. The theoretical analysis is confirmed in the same paper by use of a separately presented memristor emulator circuit from Ref. [17]. However, the results in the analysis is based on a memristor which exhibits a linear relationship between memductance and flux. This is obviously not the case for many memristors, such as the simplest case of a flux-controlled switching memristor presented in Ref. [18] where flux is controlled independent of memductance. As such, there is only a very narrow scope of memristors which the research in Ref. [16] applies to. The results in Ref. [18] served to broaden this assumption to ideal switching memristors which operate in two states, and obtain new results based on the same constitutive relation equations. This chapter dissects the results in Ref. [18] and presents them in a more comprehensive format, with the use of fundamental memristor theory to form the basis of the analysis to produce valid results. As such, the findings in this chapter can be applied more broadly and yet maintain the complex behavior which makes the memristor so attractive. The theoretical analysis and analytical solutions provide for novel memductance behavior in terms of flux, charge, voltage and current of ideal memristors. In the process, it is proven that the memristor closure theorem continues to stand for coupled memristors [19].

2. Coupled memristors

The two types of ideal memristors considered are charge controlled or flux controlled [2]. The relationship between current and voltage of a charge controlled memristor is expressed by

$$V(t) = M(q)i(t), \tag{1}$$

where t is time, $v(t)$ is voltage, $q(t)$ is charge and $M(q)$ is memristance. In its derivative form, memristance can be defined as

$$M(q) = d\varphi(q)\Big/_{dq}, \tag{2}$$

where $\phi(q)$ is flux (the time integral of voltage $v(t)$). Contrastingly, the current of a flux controlled memristor is

$$i(t) = W(\varphi)v(t), \tag{3}$$

where $W(\phi)$ denotes the memductance and

$$W(\varphi) = dq(\varphi)\Big/_{d\varphi}. \tag{4}$$

The memductance W is the slope of the q-ϕ curve, which is a characteristic embedded into the memristor at the time of fabrication.

Flux ϕ and charge q are two intrinsic state variables which affect memductance. Two memristors can be coupled by either flux or charge as shown in **Figures 1** and **2**.

If two flux controlled memristors are considered, the ideal coupled memristive systems can be defined by the following set of equations,

$$i_1(t) = W_1(\varphi_1, \varphi_2)v_1(t), \tag{5a}$$

$$i_2(t) = W_2(\varphi_1, \varphi_2)v_2(t), \tag{5b}$$

$$d\varphi_1/dt = v_1(t), d\varphi_2/dt = v_2(t). \tag{5c}$$

While a general rule cannot be ascertained which would be applicable for all ideal memristors, the most appropriate manner in approaching the task of modeling a pair of coupled memristors is to provide a procedural methodology instead. This is done by way of example with use of a particular type of switching memristor, complete with a known q-ϕ relationship.

Instead of assuming a linear relationship between memductance and flux as in Ref. [15], it is more appropriate to consider the ideal memristor proposed in Ref. [4], and derive the associated relationship between flux and memductance from a given q-ϕ relationship. An example of an ideal switching memristor is shown below in **Figure 3**, and the response of the memristor can be completely described by the q-ϕ curve displayed.

For the purposes of this paper, this example of an ideal switching memristor is completely characterized by the following equations:

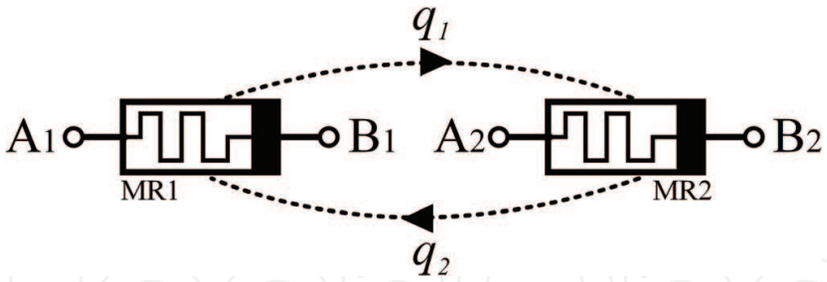

Figure 1. Dual charge coupled memristors.

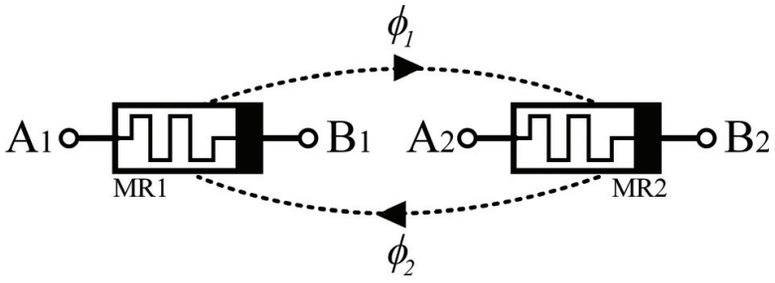

Figure 2. Dual flux coupled memristors.

http://dx.doi.org/10.5772/intechopen.69327

$$\varphi(t) = 0.8(1 - \cos t) - 0.4, \tag{6a}$$

$$q(t) = 0.01\varphi(t) + 0.04\,|\varphi(t) + 0.25| - 0.04\,|\varphi(t) - 0.25|. \tag{6b}$$

Given Eqs. (6a) and (6b), the memductance value can be derived from Eq. (4) and is graphed below in **Figure 4**.

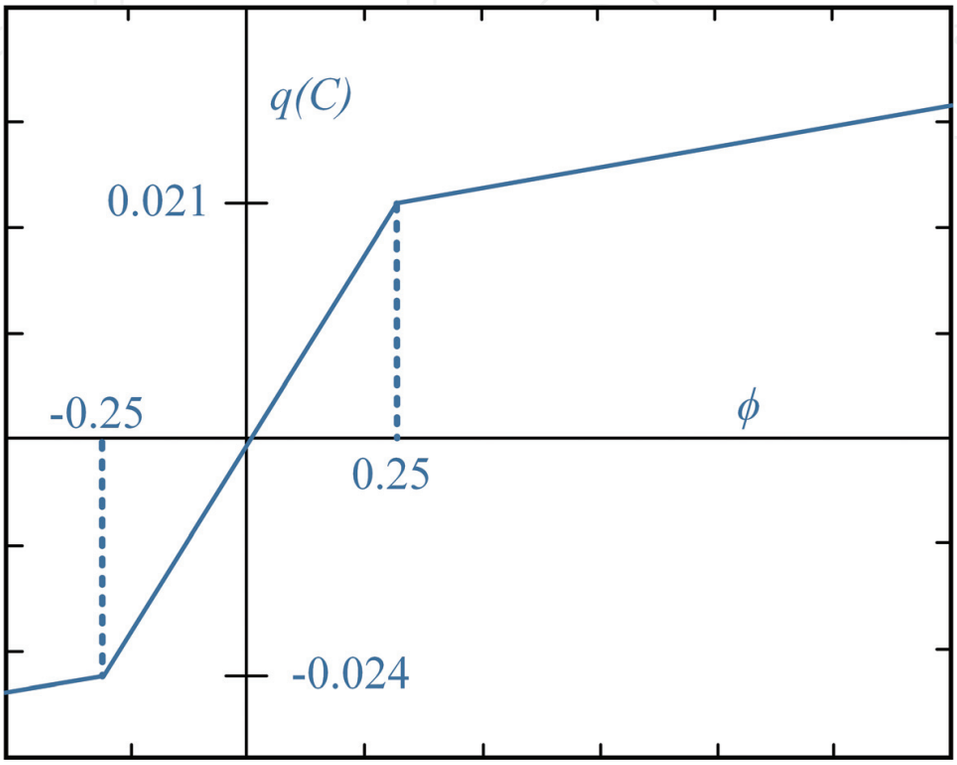

Figure 3. The q-ϕ relationship for an ideal switching memristor proposed in Ref. [4].

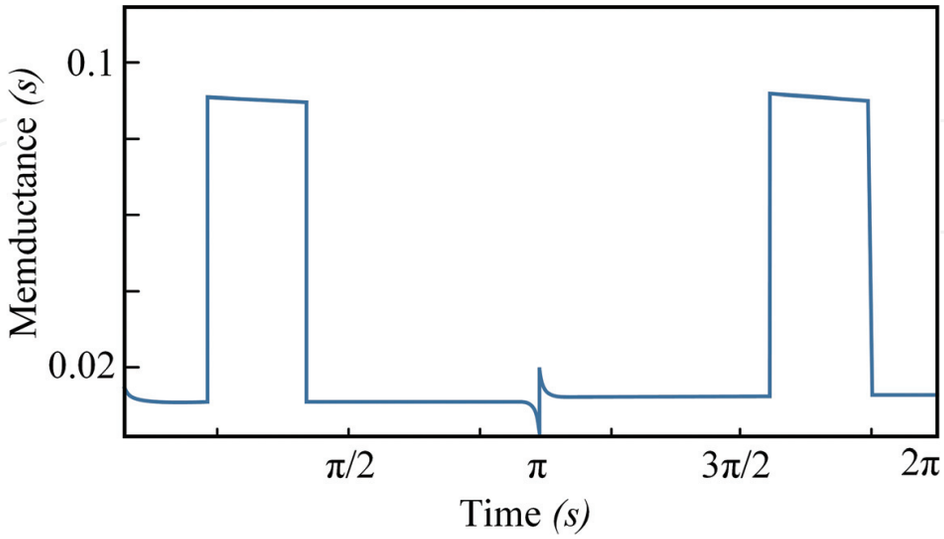

Figure 4. The memductance curve as a function of time derived from Eqs. (4), (6a), and (6b) displays how a memristor with a three part piecewise linear relationship between flux can switch between high and low current states.

The memductance can be approximated by

$$W = \begin{cases} \alpha, & |\varphi| < |\varphi_t| \\ \beta, & |\varphi_t| < |\varphi| < |\varphi_{max}| \end{cases} \tag{7}$$

where α is a constant representing the high memductance state, β is the low memductance state, ϕ_{max} is the maximum value of flux for a given sinusoidal voltage input (which in this particular case can be calculated by substituting $t = \pi$ rads into Eq. (6a) where $\phi_{max} = 1.2$), and ϕ_t is a certain threshold of flux where both current and memductance become discontinuous (in this case $\phi_t = 0.4$). Once again, it is reiterated that even though q and ϕ are referred to as charge and flux, they are not necessarily associated with real physical charge and flux in the way they are in classical conductors and inductors.

If this specific type of memristor is purely flux coupled with an identical memristor (without any other composite connections), and assuming the simple case of a first order mathematical model of coupling, the individual memductance of each device can be ascertained from Eqs. (5) and (7) as

$$W_1(\varphi_1, \varphi_2) = \begin{cases} \alpha_1 + \kappa_2\varphi_2, & |\varphi_1| < |\varphi_t| \\ \beta_1 + \kappa_2\varphi_2, & |\varphi_t| < |\varphi_1| < |\varphi_{max}| \end{cases} \tag{8a}$$

$$W_2(\varphi_2, \varphi_1) = \begin{cases} \alpha_2 + \kappa_1\varphi_1, & |\varphi_1| < |\varphi_t| \\ \beta_2 + \kappa_1\varphi_1, & |\varphi_t| < |\varphi_1| < |\varphi_{max}| \end{cases} \tag{8b}$$

The coupling strength between these two memristors is reflected by the coupling coefficients κ_1 and κ_2 which can be tuned based on physical factors in fabrication. Therefore, the two memristors can be tightly or loosely coupled depending on the values of κ_1 and κ_2.

A solvable equation with physical meaning requires assumptions about the physical behavior of the memristors. By considering the special case of identical excitations and voltage history (alternatively, the same initial conditions), and allowing for $\alpha_1 = \alpha_2 = \alpha$, $\beta_1 = \beta_2 = \beta$, and $\kappa_1 = \kappa_2 = 0.1$ (which can be precisely achieved by fabrication) the constitutive relations are used to identify behavior unachievable by the lone memristor. Memductance after coupling effects in Eq. (8) can be attained by summing flux from Eq. (6a) with memductance from Eq. (7). Current is recalculated to take into account the effect from coupling due to the composite memristor. This can be done by taking the time derivative of Eq. (6a) which is the driving voltage source, and substituting it into Eq. (3).

The *I-V* characteristic plane can be mapped by considering the two purely coupled memristors (without any other connections) as a single device. This procedure is carried out with two identical ideal flux-coupled memristors represented by **Figure 3** and configured as in **Figure 2**, to provide the *I-V* characteristics below.

When compared to the original hysteresis loop of just one of the two memristors, there are two notable differences: (i) the current spans a larger range of values due to the additive effect of ϕ_2 on i_1 (conversely, ϕ_1 has an identical effect on i_2), and (ii) the single memristor has two different

slope values which correlate to two different states, whereas in the coupled case, there are infinite states.

Despite this being the result of a specific type of switching memristor, it is reasonable to conclude these two changes will occur in all cases of purely coupled switching memristors.

This result can be exploited in neural circuits where synaptic spikes have more complexity than mere 'ON-OFF states'. On the other hand, it may have an undesirable effect on memristive logic gates where having two states is essential for functionality. Necessary physical precautions must be taken in order to minimize the values of κ_1 and κ_2 for such processes, and to additionally account for excessive current passage through the memristor due to coupling. But if logic gates were to be extended beyond high and low states, then the multiple states of the memristor could be harnessed into a multi-level logic gate on a nanometer scale.

3. Coupled memristors in serial connections

Two different configurations of serially connected memristors exist according to polarity combinations. The same approximation of the ideal memristors will apply to this section in the same form as in Eq. (7).

3.1. Serial connection with identical polarities

Connecting terminal B_1 to A_2 allows for a serial circuit structure for two memristors in identical polarities as shown in **Figure 5**.

Applying Kirchhoff's voltage Law (KVL) and equating the current through both memristors, the voltage across and current through A_1 and B_2 can be written as

$$v_{12}(t) = v_1 + v_2, \tag{9a}$$

$$i(t) = W_1(\varphi_1, \varphi_2)v_1(t) = W_2(\varphi_2, \varphi_1)v_2(t). \tag{9b}$$

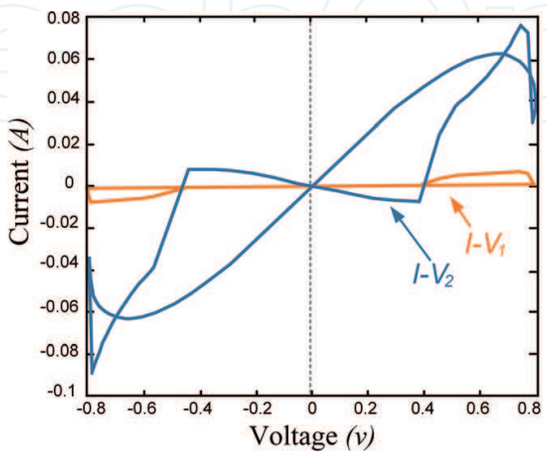

Figure 5. Memristors serially coupled with identical polarity configuration.

Integrating both sides of Eq. (9a) leads to Eq. (10a), and substituting Eq. (8) into Eq. (9b) leads to Eq. (10b),

$$\varphi_{12}(t) = \varphi_1 + \varphi_2 \tag{10a}$$

$$\begin{aligned} i &= v_1\left(\begin{cases} \alpha_1 + \kappa_2\varphi_2, & |\varphi_1| < |\varphi_t| \\ \beta_1 + \kappa_2\varphi_2, & |\varphi_t| < |\varphi_1| < |\varphi_{max}| \end{cases}\right) \\ &= v_2\left(\begin{cases} -\alpha_2 + \kappa_1\varphi_1, & |\varphi_1| < |\varphi_t| \\ -\beta_2 + \kappa_1\varphi_1, & |\varphi_t| < |\varphi_1| < |\varphi_{max}| \end{cases}\right) \end{aligned} \tag{10b}$$

From Eqs. (5), (9a) and (10), and by considering the special case of $\alpha_1 = \alpha_2 = \alpha$, $\beta_1 = \beta_2 = \beta$, $\kappa_1 = \kappa_2 = \alpha$, the following set of differential equations are obtained:

$$d\varphi_1\Big/_{dt} = v_{12}(1 + \varphi_1)\Big/_{(2 + \varphi_{12})} \tag{11a}$$

$$d\varphi_2\Big/_{dt} = v_{12}(1 + \varphi_2)\Big/_{(2 + \varphi_{12})} \tag{11b}$$

Eq. (11) reflects the complexity of memristive coupling: the derivatives of ϕ_1 and ϕ_2 are both functions of themselves and one another. If ϕ_1 changes due to an excitation voltage, a change in ϕ_2 is observed based on Eq. (11b). The change in ϕ_2 will affect ϕ_1 (independently of the initial excitation change), which goes back around to affect ϕ_2 and so on. The complex behaviors of memristive coupling are reflected in the way the flux variables are entangled in the solution of one another. Time dependence can therefore be eliminated in order to produce a solvable equation by substituting Eqs. (9a) and (10a) into Eq. (11), and dividing Eq. (11a) by Eq. (11b) (resp. Eq. (11b) by Eq. (11a)), which results in

$$d\varphi_1\Big/_{d\varphi_2} = (1 + \varphi_2)\Big/_{(1 + \varphi_1)}. \tag{12}$$

This can be analytically solved to give

$$\varphi_1(\varphi_2) = c_1\varphi_2 + c_1 - 1 \tag{13a}$$

$$\varphi_2(\varphi_1) = c_2\varphi_1 + c_2 - 1, \tag{13b}$$

where c_1 and c_2 are both constants calculable based on pre-determined initial conditions of ϕ_1 and ϕ_2. A number of cases are considered in order to ascertain a general rule for the values of c_1 and c_2 in terms of initial conditions. All of these cases can easily be created by simply biasing the relevant memristor with a rectangular voltage pulse over a given time in order to adjust the initial flux conditions. It is also worth noting that constants c_1 and c_2 can be changed at any time by switching off the driving voltage and re-biasing the memristor values. If it is assumed the flux

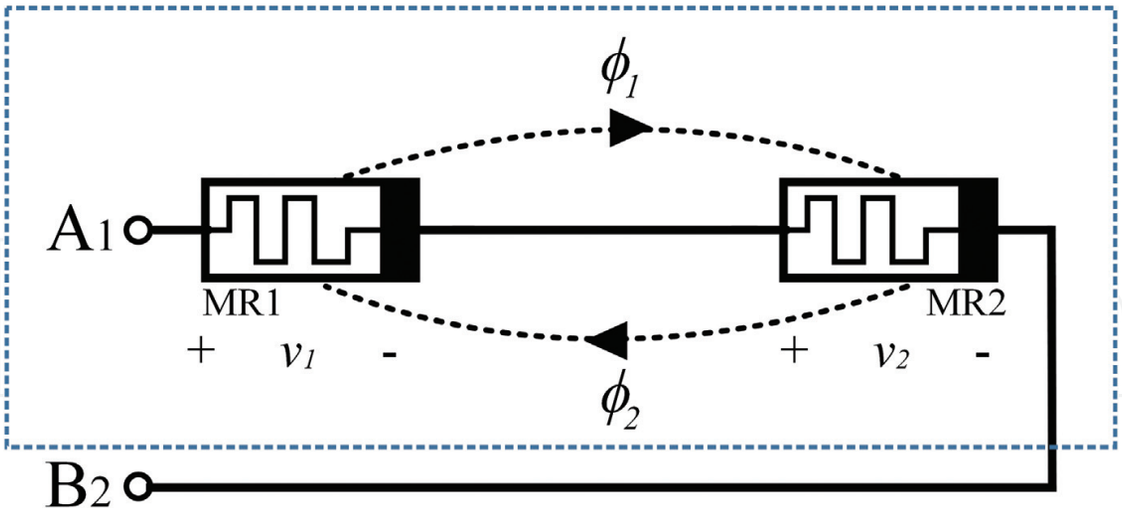

Figure 6. As initial condition u changes, c_1 produces a reciprocal curve and c_2 displays linear behavior.

state of MR1 from **Figure 5** is initially at $\phi_1 = 0$ while the flux in MR2 ϕ_2 is varied, a general rule regarding the relationship between c_1 and c_2 with initial condition of MR2 $\phi_2(\phi_1 = 0) = u$ is developed and graphed in **Figure 6**:

$$c_1 = {}^1/(1+u) \tag{14a}$$

$$c_2 = u + 1 \tag{14b}$$

3.1.1. Serial Case 1: parity at u = 0, u = −2

Substituting $u = 0$ into Eq. (13b) results in the simple solution of $c_1 = c_2 = 1$, or $\phi_1(\phi_2) = \phi_2$ and $\phi_2(\phi_1) = \phi_1$. Substituting this into Eq. (10a) results in parity between the flux value of each memristor: $\phi_1 = \phi_2 = {}^1/_2\phi_{12}$. Where $u = -2$, $c_1 = c_2 = -1$, $\phi_1(\phi_2) = \phi_2 - 2$ and $\phi_2(\phi_1) = \phi_1 - 2$.

3.1.2. Serial Case 2: u = 0 → ∞, u = −1 → −∞

As u increases from 0, c_2 linearly approaches ∞, and $c_1 \to 1/\infty$. As an example, if $u = 1$, then the constants $c_1 = {}^1/_2$, $c_2 = 2$, and $\phi_1(\phi_2) = {}^1/_2\phi_2 - {}^1/_2$, $\phi_2(\phi_1) = 2\phi_1 + 1$. By assuming the excitation voltage is a sinusoidal input, the peak-to-peak amplitude of flux across ϕ_1 is half of that in Serial Case 1, whereas ϕ_2 has quadrupled. A tug-of-war of sorts occurs between ϕ_1 and ϕ_2: as ϕ_2 increases, ϕ_1 decreases. Conversely, as u decreases from −2, $c_2 \to -\infty$, and $c_1 \to -1/\infty$.

3.1.3. Serial Case 3: u = 0 → −1, u = −2 → −1

This case behaves similarly to Case 2, but reversed. As u decreases from 0 towards −1, $c_1 \to \infty$. As u increases from −2 towards −1, $c_1 \to -\infty$. It is asymptotical at $u = -1$, while c_2 behaves

linearly and passes through 0 at $u = -1$. The advantage of this case over Case 2 is that much less power is required to bias a memristor between these values in order to attain a flux value that approaches infinity. In other words, given a memristor without state boundary conditions, one can control it to behave like a regular resistor instead if so desired.

3.1.4. Serial Case 4: $u = -1$

Mathematically, there is no solution for c_1 as it approaches $\pm\infty$ (depending on which side it approaches in accordance with **Figure 6**). Hence, in theory, MR1 is never in equilibrium when the two memristors are serially flux coupled with identical polarities, where the initial flux value of MR2 is -1 and MR1 is 0. Eq. (13a) shows that as $c_1 \to \infty$, $\phi_1 \to \infty$. If this behavior is mapped against the given charge-flux relationship of the memristor characterized by **Figure 3**, the top segment of the memristor is a straight line. Therefore, after a sufficiently long time interval, ϕ_1 tends to the breakpoint and the memristor becomes equivalent to a resistor with a resistance of the inverse slope of the final segment (resp. where $c_1 \to -\infty$, $\phi_1 \to -\infty$ and the memristor becomes equivalent to a resister with the value of the inverse slope of the first segment of the q–ϕ curve).

The effect seen here with flux approaching an infinite value is identical to an ideal memristor being connected to a DC source. A constant non-periodic voltage source will also result in flux tending indefinitely towards $\pm\infty$, due to the integral relationship implied by Eq. (5c).

This result will not hold true for all ideal memristors [4]. If the memristor was defined by a polynomial $q - \phi$ curve, while $\phi \to \pm\infty$, $\frac{dq}{dt} = i(t) \to \pm\infty$. This implies that the memristor in question does not have a dc *V-I* curve, and in practice, the memristor would burn out long before the current became too large. This must also be considered in both Case 2 and Case 3, where current values can potentially go beyond the memristors capacity.

Given a sinusoidal voltage for v_{12} from Eq. (9a) in the general form of

$$v_{12} = A\sin(2\pi f t), \tag{15}$$

where A is the amplitude of v_{12}, both ϕ_1 and ϕ_2 will take on a sinusoidal form as well, and functions for memductance, voltage and flux can be found in terms of time, initial conditions and amplitude A—all of which can easily be predetermined.

For the sake of both attaining a meaningful solution and demonstration, flux is first determined as a function of time where the term from Eq. (15) ($2\pi f$) is assumed to be 1 rad. This simplification yields

$$\varphi_2(t) = -\gamma\cos(t) + u, \tag{16a}$$

where γ is the amplitude of ϕ_2, and if Eq. (16a) is substituted into Eq. (13a) results in

$$\varphi_1(t) = -c_1\gamma\cos(t) + (c_1 u + c_1 - 1). \tag{16b}$$

Substituting Eq. (16) into Eqs. (9a) and (5c) results in

$$v_{12} = v_1 + v_2 = (\gamma + c_1\gamma)\sin(t) \tag{17}$$

Alternatively,

$$\gamma + c_1\gamma = A \tag{18}$$

And substituting Eqs. (14) and (18) into Eq. (16) gives

$$\varphi_1(t) = -A/(2+u)\cos(t) \tag{19a}$$

$$\varphi_2(t) = -A(1+u)/(2+u)\cos(t) + u \tag{19b}$$

The assumption used in deriving Eq. (14) was that the initial condition of MR1 was $\phi_1 = 0$, at which time $\phi_2 = u$. Consider when $t = \pi/2$ *s:* ϕ_1 is indeed 0, and ϕ_2 is reduced to the initial condition u.

To find memductances W_1 and W_2 after serial coupling Eq. (19) is substituted into Eq. (8) to give

$$W_1 = \begin{cases} \alpha_1 - \kappa_1\left((A(1+u))/(2+u)\cos(t) + u\right), & |\varphi_1| < |\varphi_t| \\ \beta_1 - \kappa_1\left((A(1+u))/(2+u)\cos(t) + u\right), & |\varphi_t| < |\varphi_1| < |\varphi_{max}| \end{cases} \tag{20a}$$

$$W_2 = \begin{cases} \alpha_2 - \kappa_2\left(A/(2+u)\cos(t)\right), & |\varphi_1| < |\varphi_t| \\ \beta_2 - \kappa_2\left(A/(2+u)\cos(t)\right), & |\varphi_t| < |\varphi_1| < |\varphi_{max}| \end{cases} \tag{20b}$$

The memductance (and by extension, current) can therefore be adjusted based on u. Biasing the initial state of MR2's flux for a desired value allows the two memristors to behave harmoniously like a pair of complementary variable switching resistors (while still maintaining the high-low voltage states of the single memristor represented in **Figure 4**).

When $u = 0$, and in the special case of $\alpha_1 = \alpha_2$, $\beta_1 = \beta_2$, and $\kappa_1 = \kappa_2$, Eq. (20) shows that $W_1 = W_2$ and $v_1 = v_2 = ½v_{12}$. As u increases from 0, W_1 increases and W_2 decreases. This is agreeable with Serial Case 2 of **Figure 6**: ϕ_2 increases and is the cause for coupling with MR1 which results in the increase of W_1 (resp. the decrease of ϕ_1 as u increases is the cause of the decrease in W_2). The same methodology applies for the other cases too.

While a memristor has a variable resistance by its very definition, this variation is limited by the value of $d\phi/dq$ according to the charge-flux curve. However, when two memristors have an additional parameter u which contributes to this variation, the two serially flux coupled memristors behave as variable memristors which can be adjusted based on Eq. (20).

Figure 7 represents memductances derived from Eq. (18) at $\kappa_1 = \kappa_2 = 0.02$, $\alpha_1 = \alpha_2 = 0.1$, $\beta_1 = \beta_2 = 0.01$, and as shown in Serial Case 1, when $u = 0$ the two memristors operate with identical flux values which leads to identical memductance values $W_1 = W_2 = W$. When the

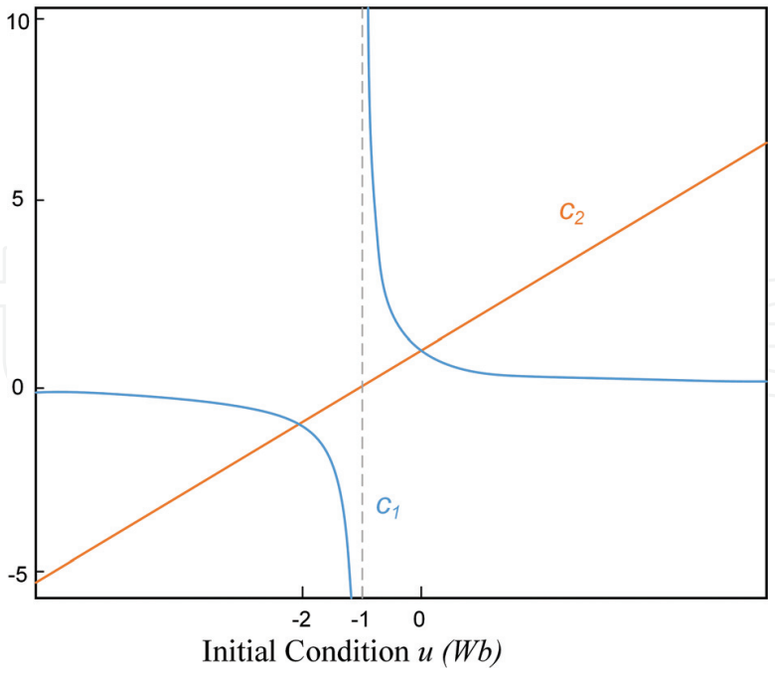

Figure 7. The memductance curve of serially coupled memristors, $u = 0$ for W, and $u = 0.02$ for W_1 and W_2.

initial condition of MR2 is changed to $u = 0.02$, the memductance of MR1 shifts upwards while the memductance of MR2 is approximately the same as W.

3.2. Serial connection with opposite polarities

Following a similar procedure to above where one of two memristors in **Figure 8** are flipped such that either terminals A_1 and A_2, or B_1 and B_2 are connected, as shown in **Figure 9**, applying KVL to Eqs. (5) and (8) yields

$$\begin{aligned} i &= v_1 \begin{cases} \alpha_1 - \kappa_2\varphi_2, & |\varphi_1| < |\varphi_t| \\ \beta_1 - \kappa_2\varphi_2, & |\varphi_t| < |\varphi_1| < |\varphi_{max}| \end{cases} \\ &= v_2 \begin{cases} -\alpha_2 + \kappa_1\varphi_1, & |\varphi_1| < |\varphi_t| \\ -\beta_2 + \kappa_1\varphi_1, & |\varphi_t| < |\varphi_1| < |\varphi_{max}| \end{cases} \end{aligned} \tag{21}$$

and substituting Eq. (5c) along with the same assumptions $\beta_1 = \beta_2 = \beta$, $\alpha_1 = \alpha_2 = \kappa_1 = \kappa_2 = \alpha$ into Eq. (21) results in the following differential equations

$$d\varphi_1/dt = -(1 + \varphi_1)/(1 - \varphi_2) \tag{22a}$$

$$d\varphi_2/dt = -(1 - \varphi_2)/(1 + \varphi_1), \tag{22b}$$

which solving simultaneously assuming initial conditions $\phi_1(t) = \phi_2(t) = \phi(0)$ results Eqs. (23a) and (23b), pictorially represented in **Figure 10**.

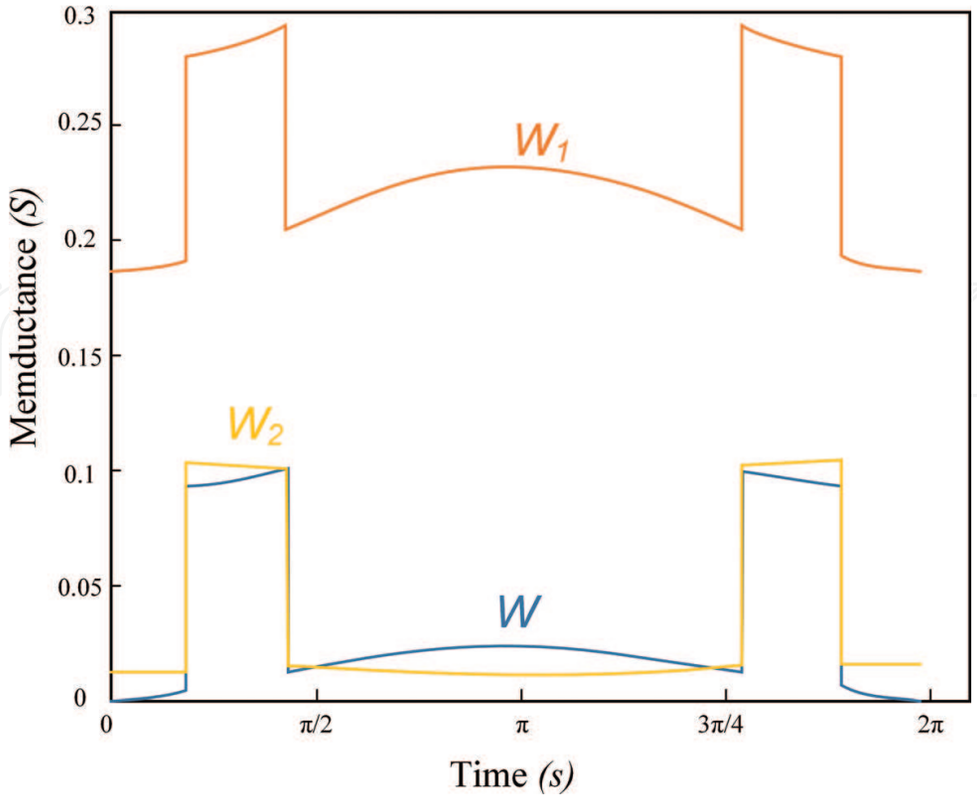

Figure 8. The *I-V* characteristic of two identical flux-coupled memristors shown in **Figure 2** denoted $I\text{-}V_2$ compared to the *I-V* characteristic of just one memristor $I\text{-}V_1$.

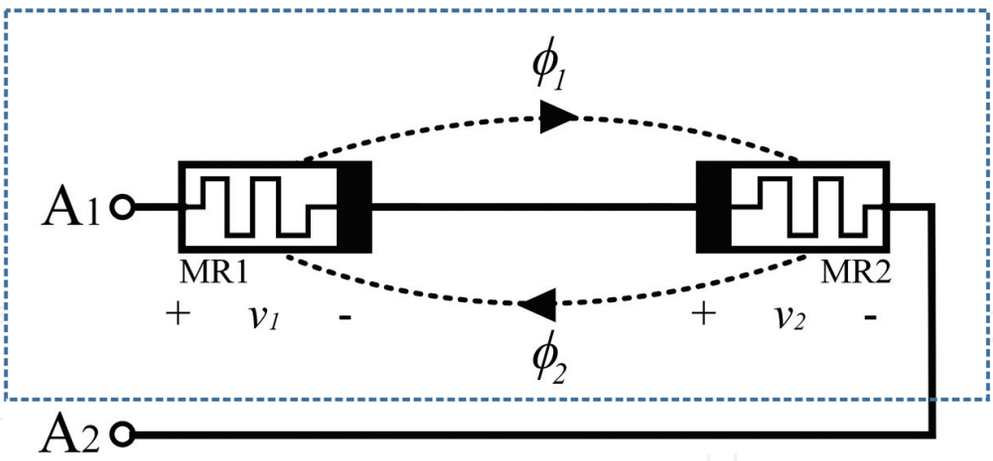

Figure 9. Memristors serially coupled with opposite polarity configuration.

$$\varphi_1 = \frac{1}{2}(-1 + e^{2t}), \tag{23a}$$

$$\varphi_2 = 1/2 - (e^{-2t})/2 \tag{23b}$$

Therefore, memductance of the individual memristor can be obtained by substituting Eq. (23) into Eq. (8), and assuming $\beta_1 = \beta_2 = \beta$, $\alpha_1 = \alpha_2 = \alpha$, $\kappa_1 = \kappa_2 = \kappa$.

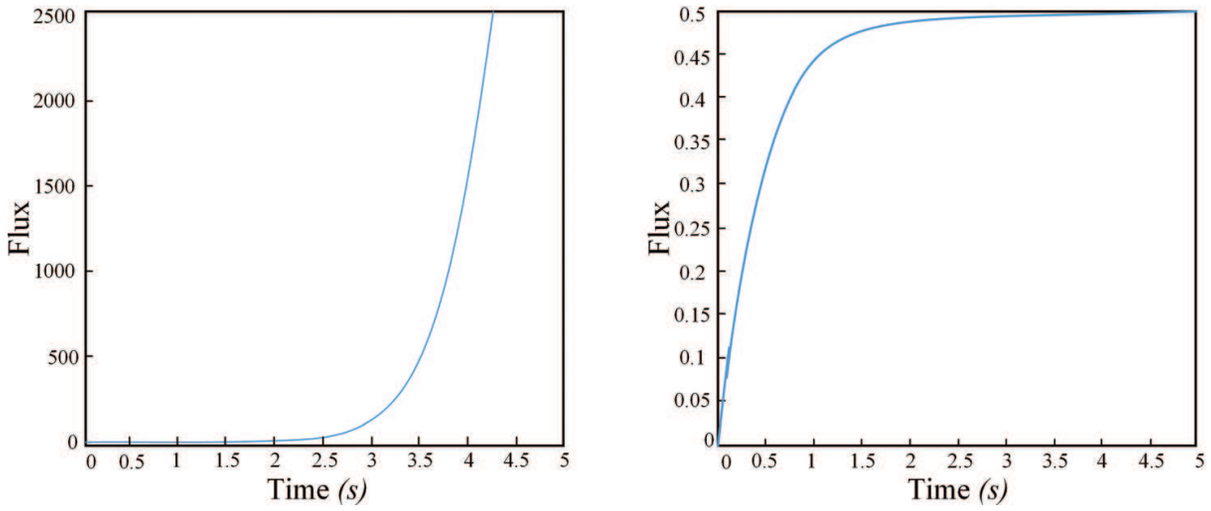

Figure 10. Flux variation with time in anti-serial connection: figure on left displaying $\phi_1(t)$ from Eq. (23a); figure on right figure showing $\phi_2(t)$ from Eq. (23b).

$$W_1(\varphi_1, t) = \begin{cases} \alpha + \kappa\left(\frac{1}{2} - \frac{e^{-2t}}{2}\right), & |\varphi_1| < |\varphi_t| \\ \beta + \kappa\left(\frac{1}{2} - \frac{e^{-2t}}{2}\right), & |\varphi_t| < |\varphi_1| < |\varphi_{max}| \end{cases} \tag{24a}$$

$$W_2(\varphi_2, t) = \begin{cases} \alpha + \frac{\kappa}{2}(-1 + e^{2t}), & |\varphi_2| < |\varphi_t| \\ \beta + \frac{\kappa}{2}(-1 + e^{2t}), & |\varphi_t| < |\varphi_2| < |\varphi_{max}|. \end{cases} \tag{24b}$$

In **Figure 10**, $\phi_1(t)$ never stops, but increases to $+\infty$. Hence, just as calculated in Serial Case 4 of 'Serial Connection with Identical Polarities', one of two ideal memristors can never be in equilibrium when coupled in anti-serial connection.

Once again, this behavior is mapped against the given charge-flux relationship of the switching memristor characterized by the shape of the curve in **Figure 3**. The first and final segments of the curve are theoretically non-ending straight lines, and thus, after a voltage pulse is applied for a sufficiently long time interval to increase flux far beyond the upper breakpoint $\phi_1 = 0.25$ (resp. a negative voltage pulse to decrease flux beyond the lower breakpoint $\phi_1 = -0.25$), the memristor becomes the equivalent of a resistor with the resistance value of the inverse slope of the final segment.

This behavior is considered comparatively against a single ideal memristor excited by a DC voltage. Suppose a battery with voltage E *volts* is connected across this memristor at $t = 0$. Where $E > 0$, $\phi(t)$ tends towards $+\infty$. Just as in the case of MR1 of the two anti-serially flux-coupled memristors, the DC-excited memristor is equivalent to a resistor with value of the inverse of the charge-flux slope.

Ignoring threshold switching effects, the memductance of MR1 reaches a steady state value while MR2 never achieves stability and instead tends towards a perfect conductor. However,

these memristors will not display this behavior independently and so it is more practical to consider the two memristors as a single black box device. Equivalent memductance across A_1 and A_2 can be numerically obtained as $W_1W_2/(W_1+W_2)$ based on values of α, β and κ.

4. Coupled memristors in parallel connections

Two different configurations of parallel connected memristors exist according to polarity combinations, just as is the case with serially connected memristors. The same approximation of the ideal memristors will apply to this section in the same form as in Eq. (7). The first case to consider where memristors are configured with identical polarities is depicted in **Figure 11**.

4.1. Parallel connection with identical polarities

The current passing through A_1 and B_2 as well as flux ϕ_{12} can be derived from Kirchhoff's Current Law (KCL) and Eq. (8),

$$i = i_1 + i_2,\ \varphi_{12} = \varphi_1 + \varphi_2, \tag{25}$$

$$i = \begin{cases} v_1(\alpha_1 + \kappa_2\varphi_2) + v_2(\alpha_2 + \kappa_1\varphi_1),\ |\varphi_{12}| < |2\varphi_t| \\ v_1(\beta_1 + \kappa_2\varphi_2) + v_2(\beta_2 + \kappa_1\varphi_1), |2\varphi_t| < |\varphi_{12}| < |2\varphi_{max}| \end{cases} \tag{26}$$

Integration both sides of Eq. (24) yields

$$q = \begin{cases} (\alpha_1 + \alpha_2)\varphi_{12} + \frac{1}{2}(\kappa_1 + \kappa_2)\varphi_{12}^2,\ |\varphi_{12}| < |2\varphi_t| \\ (\beta_1 + \beta_2)\varphi_{12} + \frac{1}{2}(\kappa_1 + \kappa_2)\varphi_{12}^2,\ |2\varphi_t| < |\varphi_{12}| < |2\varphi_{max}| \end{cases} \tag{27}$$

Memductance can accordingly be calculated,

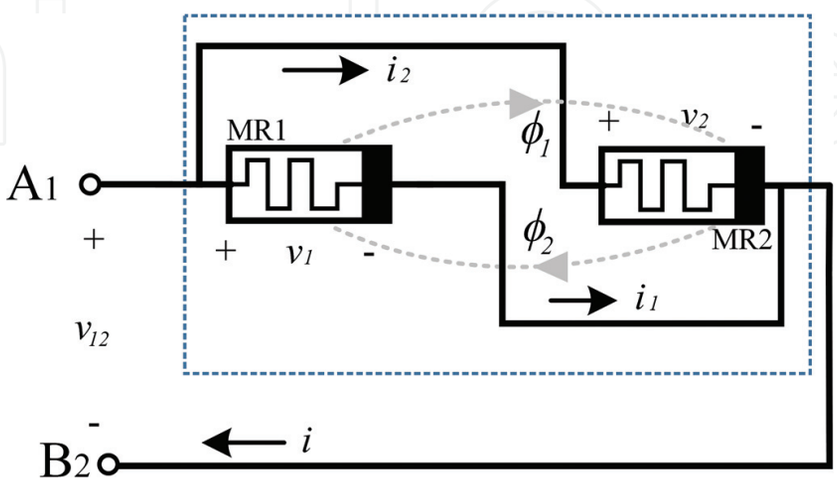

Figure 11. Coupled memristors connected in parallel with identical polarity configuration.

$$W_{12}(\varphi_{12}) = \frac{dq(\varphi_{12})}{d\varphi_{12}} = \begin{cases} (\kappa_1 + \kappa_2)\varphi_{12} + \alpha_1 + \alpha_2, \ |\varphi_{12}| < |2\varphi_t| \\ (\kappa_1 + \kappa_2)\varphi_{12} + \beta_1 + \beta_2, \ |2\varphi_t| < |\varphi_{12}| < |2\varphi_{max}| \end{cases} \tag{28}$$

In this case the variation between the memductance and flux ϕ_{12} is dependent on the total of the coupling coefficient values, κ_1 + κ_2. While the total coupling coefficient is positive, memductance is in positive proportion to the excitation flux: a higher flux will result in higher memductance. Conversely, when the total coupling coefficient is negative, the memductance will linearly decrease with the increase of flux. It can be clearly observed from Eq. (28) that flux coupled memristors in parallel connection behave as a new flux controlled memristor, with the equivalent memductance equivalent to the sum of the individual memductances.

4.2. Parallel connection with opposite polarities

A similar procedure can be used in order to ascertain the behavior of anti-parallel connected flux coupled memristors.

In the case shown in **Figure 12**, the current and flux across terminals A_1 and A_2 are also derived from KCL with the same relationship as in Eq. (25). When considered with respect to Eqs. (3) and (8), and using similar mathematical derivations to the previous sections the following result is obtained:

$$i(t) = \begin{cases} v_1(\alpha_1 - \kappa_2\varphi_2) + v_2(\alpha_2 + \kappa_1\varphi_1), \ |\varphi_{12}| < |2\varphi_t| \\ v_1(\beta_1 - \kappa_2\varphi_2) + v_2(\beta_2 + \kappa_1\varphi_1), |2\varphi_t| < |\varphi_{12}| < |2\varphi_{max}| \end{cases} \tag{29}$$

Integrating both sides of Eq. (29) results in a coupled charge-flux relationship as shown below,

$$q = \begin{cases} (\alpha_1 + \alpha_2)\varphi_{12} + \frac{1}{2}(\kappa_1 - \kappa_2)\varphi_{12}^2, \ |\varphi_{12}| < |2\varphi_t| \\ (\beta_1 + \beta_2)\varphi_{12} + \frac{1}{2}(\kappa_1 - \kappa_2)\varphi_{12}^2, \ |2\varphi_t| < |\varphi_{12}| < |2\varphi_{max}| \end{cases} \tag{30}$$

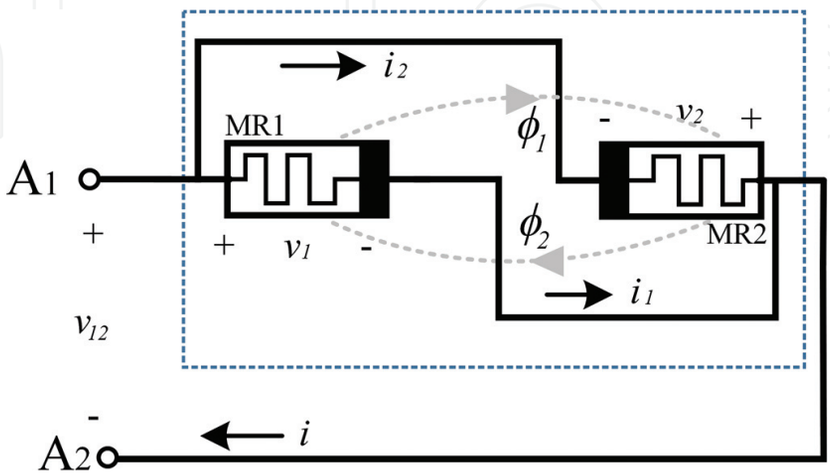

Figure 12. Coupled memristors connected in parallel with opposite polarity configuration.

http://dx.doi.org/10.5772/intechopen.69327

Finally, substituting Eq. (30) into Eq. (4) gives the total memductance of the coupled memristors in parallel connection:

$$W_{12}(\varphi_{12}) = \frac{dq(\varphi_{12})}{d\varphi_{12}} = \begin{cases} (\kappa_1 - \kappa_2)\varphi_{12} + \alpha_1 + \alpha_2, & |\varphi_{12}| < |2\varphi_t| \\ (\kappa_1 - \kappa_2)\varphi_{12} + \beta_1 + \beta_2, & |2\varphi_t| < |\varphi_{12}| < |2\varphi_{max}| \end{cases} \tag{31}$$

For the uncoupled case of $\kappa_1 = \kappa_2 = 0$, the parallel memristors operate as a new memristor where the memductance states (α_1, α_2, β_1, β_2) are additive, and all contribute towards the total coupled memductance. This particular aspect of the relationship is common to both parallel connection combinations when polarity is changed. The difference between the two cases is in the effect of the coupling coefficient.

5. Conclusion

A comprehensive theoretical analysis of flux coupled memristors displays various kinds of new behaviour which are otherwise unattainable from a single memristor. The simplest case of coupling between two switching memristors is shown to have a diverse range of properties when memristors are acting in composite with each other. The results presented only consider bi-state memristors, and as such, we can expect different types of memristors with different charge-flux relationships to expand the types of dynamic behaviors exhibited, with the ability to modify the states attainable by tuning the variables associated with the coupling coefficient (such as physical proximity and device material just to name a couple of examples).

In summary, two serially connected memristors with identical polarities are shown to produce a pair of variable memristors determinable from initial conditions; two serially connected memristors with opposite polarities display behavior often displayed by memristors connected to DC sources, or otherwise resistive behavior. Parallel memristive systems are shown to produce a variation rate in terms of the coupling coefficients. This is a feature that can be determined at the time of fabrication.

Further, what has been considered in this paper is the simplest case of identical memristors with identical initial conditions. The potential application of coupled memristors, in addition to the undoubtedly interesting characteristics of arrays of coupled memristors will serve to open up new avenues of applications, and also provide for guidelines on avoiding undesirable behaviors by having fabrication plants devise methods to reduce the coupling coefficient as low as practicable where design specifications see it fit. In particular, where neural networks will see densely populated circuits which depend on memristors behaving functionally, the effects of coupling must either be mitigated to avoid unexpected and fallible outcomes. The alternative view is that memristive coupling makes it possible to have more than two states between a pair of memristors which would otherwise only be capable of being switched either on or off, and as such, if these intermediary states are quantized, then a large system of many varying states can be produced out of a mere two memristors connected compositely.

Acknowledgements

This work was supported by the Australia-Korea Foundation—Department of Foreign Affairs and Trade under the AKF00640 grant.

Author details

Jason Kamran Jr Eshraghian[1]*, Herbert H.C. Iu[2] and Kamran Eshraghian[3]

*Address all correspondence to: jeshraghian@gmail.com

1 Chungbuk National University, Cheongju, South Korea

2 University of Western Australia, Perth, Australia

3 iDataMap Corporation Pty Ltd, Adelaide, Australia

References

[1] Chua LO. Introduction to Nonlinear Network Theory. New York: McGraw-Hill; 1969

[2] Chua LO. Memristor: The missing circuit element. IEEE Transactions on Circuit Theory. 1971;**18**(5):507-519

[3] Strukov DB, Snider GS, Stewart DR and Williams RS. The missing memristor found. Nature. 2008;**453**:80-83. DOI: 10.1038/nature06932

[4] Chua LO. If it's pinched it's a memristor. Semiconductor Science and Technology. 2014;**29** (10):104001-1040042

[5] Sharifi MJ and Banadaki YM. General SPICE models for memristor and application to circuit simulation of memristor-based synapses and memory cells. Journal of Circuits, Systems and Computers. 2010;**19**(2):407-424

[6] Ho Y, Huang GM and Li P. Nonvolatile memristor memory: Device characteristics and design implications. In: IEEE/ACM International Conference on Computer-Aided Design, 2009; 2-5 Nov. 2009; 2009. pp. 485-490

[7] Yu DS, Iu HHC, Fitch AL and Liang Y. A floating memristor emulator based relaxation oscillator. IEEE Transactions on Circuits and Systems I: Regular Papers. 2014;**61**(10):2888-2896

[8] Budhathoki RK, Sah MP, Adhikari SP, Kim H and Chua LO. Composite behavior of multiple memristor circuits. IEEE Transactions on Circuits and Systems I: Regular Papers. 2013;**60**(10):2688-2700

[9] Mladenov V and Kirilov S. Analysis of the mutual inductive and capacitive connections and tolerances of memristors parameters of a memristor memory matrix. In: 2013 European Conference on Circuit Theory and Design (ECCTD); 8-12 Sept. 2013; 2013. pp. 1-4

[10] Prezioso M, Merrikh-Bayat F, Hoskins BD, Adam GC, Likharev KK, Strukov DB. Training and operation of an integrated neuromorphic network based on metal-oxide memristors. Nature. 2015;**521**:61-64. DOI: 10.1038/nature14441

[11] James AP, Fedorova I, Ibrayev T, Kudithipudi D. HTM spatial pooler with memristor crossbar circuits for sparse biometric recognition. IEEE Transactions on Biomedical Circuits and Systems. 2017;**11**(99):1-12. DOI: 10.1109/TBCAS.2016.2641983

[12] Adam GC, Hoskins BD, Prezioso M, Merrikh-Bayat F, Charkrabarti B, Strukov DB. 3-D memristor crossbars for analog and neuromorphic computing applications. IEEE Transactions on Electron Devices. 2017;**64**(1):312-318. DOI: 10.1109/TED.2016.2630925

[13] Truong SN, Pham KV, Yang W and Min KS. Sequential memristor crossbar for neuromorphic pattern recognition. IEEE Transactions on Nanotechnology. 2016;**15**(6): 922-930. DOI: 10.1109/TNANO.2016.2611008

[14] Yakopcic C, Alom MZ and Taha TM. Memristor crossbar deep network implementation based on a Convolutional neural network. In: 2016 International Joint Conference on Neural Networks (IJCNN); 24-29 July 2016; Vancouver, BC, Canada. IEEE; 2016. DOI: 10.1109/IJCNN.2016.7727302

[15] Cai W and Tetzlaff R. Beyond series and parallel: Coupling as a third relation in memristive systems. In: 2014 IEEE International Symposium on Circuits and Systems (ISCAS); 1-5 June 2014; 2014. pp. 1259-1262

[16] Yu DS, Iu HHC, Liang Y, Fernando T and Chua LO. Dynamic behavior of coupled memristor circuits. IEEE Transactions on Circuits and Systems I: Regular Papers. 2015;**62** (6):1607-1616

[17] Yu DS, Liang Y, Iu HHC, Chua LO. A universal mutator for transformations among memristor, memcapacitor and meminductor. IEEE Transactions on Circuits and Systems II: Express Briefs. 2014;**61**(10):758-762

[18] Eshraghian JK, Iu HHC, Fernando T, Yu DS, Li Z. Modelling and characterization of dynamic behavior of coupled memristor circuits. In: 2016 IEEE International Symposium on Circuits and Systems (ISCAS); 22-25 May 2016; 2016. pp. 690-693. DOI: 10.1109/ISCAS.2016.7527334

[19] Chua LO. Resistance switching memories are memristors. Applied Physics A. 2011;**102** (4):765-783. DOI: 10.1007/s00339-011-6264-9

IntechOpen